Characterization of Si_3N_4/SiO_2 planar lightwave circuits and ring resonators

Junpeng Guo*[a], G. Allen Vawter[a], Michael J. Shaw[a], G. Ronald Hadley[a], Peter Esherick[a], Anisha Jain[a], Charles R. Alford[b], and Charles T. Sullivan[a]

[a]Sandia National Laboratories, Albuquerque, NM, USA 87185-0603;

[b]L&M Technologies, Inc., Albuquerque, NM, USA 87109-5802

ABSTRACT

The large refractive index contrast between silicon nitride and silicon dioxide allows silicon nitride/dioxide planar waveguides to have a small mode size and low radiation bending loss compared with doped silicon dioxide waveguides. Small waveguide bend with low radiation loss can help make small integrated planar lightwave circuits (PLCs), and also high-Q waveguide ring resonators. This presentation will talk about the design, fabrication and characterization of low loss silicon nitride/dioxide planar waveguide devices including waveguide bend, waveguide cross, and leaky mode waveguide polarizer. The key contribution of this work is the use of the lateral mode interference (LMI) 3dB splitter to accurately measure the loss of the planar lightwave circuit devices. We will also talk about the waveguide ring resonators with silicon nitride/dioxide materials. The application for photonic biochemical sensors will also be discussed.

Keywords: Waveguide loss, lateral mode interferometer (LMI), waveguide polarizer, ring resonator.

1. INTRODUCTION

Silicon-based photonics has attracted a lot of interests in recent years[1, 2, 3]. The motivation for using silicon as substrate is mainly due to the mature silicon processing technology which has been developed for many years for CMOS devices. Silicon is a material that is chemically stable and mechanically rugged. High purity and low cost silicon wafers are widely available. Most importantly, it is possible to integrate photonic devices with microelectronic and micromechanical elements on the same wafer. Silicon and doped silicon, such as SiGe, are also good photodetector materials. Photodetectors can be fabricated in silicon wafers[4]. More recently, there has been an increasing interest in making active photonic devices, such as Er-doped waveguide amplifiers[5] and silicon light emitting devices[6,7] on silicon substrates. Attempts have been made to make silicon-based lasers[8,9,10]. Although not successful yet, the future is very promising.

Silicon-based optical waveguide devices can be fabricated with different material systems. These material systems typically use thermally grown silicon oxide and chemical vapor deposited (CVD) silicon oxide as waveguide cladding. The materials used for the waveguide core are phosphorous or germanium doped silica, silicon oxynitride, silicon nitride, and silicon. Doped silica waveguides have low refractive index contrast (0.1~ 1%) between the core and the cladding. Less than 0.01 dB/cm waveguide loss has been reported[11]. The small index contrast gives the doped silica waveguide a large guided mode profile. The large mode profile of the doped silica waveguide makes the bending loss extremely high for a small bend. In the other extreme, the large refractive index contrast of silicon in silica waveguides allow a small bend, but the waveguide loss due to interface roughness is very difficult to reduce[12, 13]. In terms of the refractive index contrast, silicon nitride and silicon oxynitride waveguides fall in between doped silica and silicon in silica waveguides.

The refractive index contrast between silicon nitride and silicon dioxide is reasonably large (2.0 vs. 1.45). This allows silicon nitride/silicon dioxide planar waveguides to have a small mode size and therefore low radiation bending loss compared with doped silicon dioxide waveguides. Small waveguide bending can help put more

Optical Components and Materials, edited by Michel J. F. Digonnet, Shibin Jiang, Proceedings of SPIE Vol. 5350 (SPIE, Bellingham, WA, 2004) · 0277-786X/04/$15 · doi: 10.1117/12.529641

photonic devices on a single silicon wafer. A six inch wafer can hold over six million photonic devices of 50x50 μm^2 size. Also, low waveguide bending loss can help make high-Q waveguide ring resonators. High-Q waveguide ring resonators have applications for photonic sensors and optical logic switch.

The activities of silicon–based photonics have been mostly for telecommunication applications in the last several years[2,14] making wavelength filters, switches, splitters, attenuators, etc. We are interested in silicon-based photonic devices primarily for sensor applications.

In this presentation, we will talk about the design, fabrication and characterization of low loss silicon nitride/dioxide planar waveguide devices including straight waveguide, waveguide bend, waveguide cross, and leaky mode waveguide polarizer. The key contribution of this work is the use of a lateral mode interference (LMI) 3 dB splitter to accurately measure the loss of the planar lightwave circuit devices. We will also talk about the waveguide ring resonators with silicon nitride/dioxide materials. The application for photonic biochemical sensors will also be discussed.

2. FABRICATION

The fabrication of silicon nitride waveguides starts with a six inch diameter polished <100> silicon wafer. A two micron silicon dioxide (SiO_2) film was grown on top of the silicon wafer using a thermal steam oxidation process. An additional three micron PECVD (plasma enhanced chemical vapor deposition) TEOS (tetraethylorthosilicate) oxide was deposited on top of the steam grown oxide producing a total of 5 microns of lower cladding SiO_2 film. A 120 nm thick silicon nitride (Si_3N_4) film was deposited on top of the PECVD TEOS silicon dioxide layer using a LPCVD process. The waveguide devices were patterned with a deep UV (245nm) photolithography mask aligner. The waveguides were etched using a reactive ion etching (RIE) process to define the waveguide core. Several techniques were used to reduce sidewall roughness after the initial RIE etching. The critical step was to oxidize and etch back the side walls of the Si3N4 channel waveguides. The upper cladding was 4.0 micron PECVD TEOS silicon dioxide.

There are two major sources for propagation loss in Si_3N_4/ SiO_2 waveguides. One is the scattering loss due to waveguide core/cladding interface roughness. Another is the absorption loss due to H-O bond in SiO_2 and H-N in Si_3N_4. The absorption in SiO_2 peaks at 1.4 micron and is of the same nature as the absorption in optical fibers. A similar absorption occurs in the Si_3N_4 but is shifted to 1.52 micron[15]. Unfortunately this absorption band peaks at the wavelength used for most applications. High-temperature annealing (1050 -1200 °C) can get rid of H-O and H-N bonds and significantly reduce the absorption loss. In our fabrication process, the wafers are annealed at 1100 °C at various processing points for over six hours.

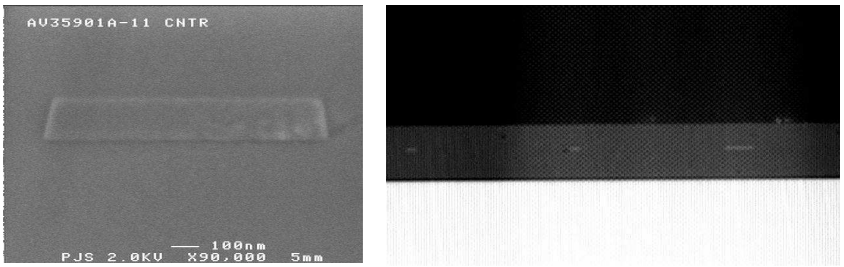

Figure 1. SEM graph of the Si_3N_4 waveguide cross-section (left) and optical microscopic picture of the Si_3N_4 waveguide cross-sections (right).

3. DESIGN AND CHARACTERIZATION

Before designing the silicon nitride waveguide, we deposited thin layers of SiO_2 and Si_3N_4 on silicon wafers and measure their indices of refraction at 1550 nm using a prism coupled thin film characterization instrument. The measured index of refraction of PECVD TEOS SiO_2 is 1.448 at 1550 nm. The measured index of refraction of annealed LPCVD deposited Si_3N_4 is 1.98 at 1550 nm. The annealed LPCVD deposited Si_3N_4 film has about 0.5% lower index of refraction than unannealed Si_3N_4 film. We used the measured refractive index data to design the waveguide. In our design, the cross section of the silicon nitride waveguide core was 1.2 micron by 0.12 micron. This cross section guarantees that it is operated in the single fundamental mode at a wavelength of 1550nm. Figure 2 is the calculated electric field mode profile of the single mode waveguide. The effective mode index is 1.4773.

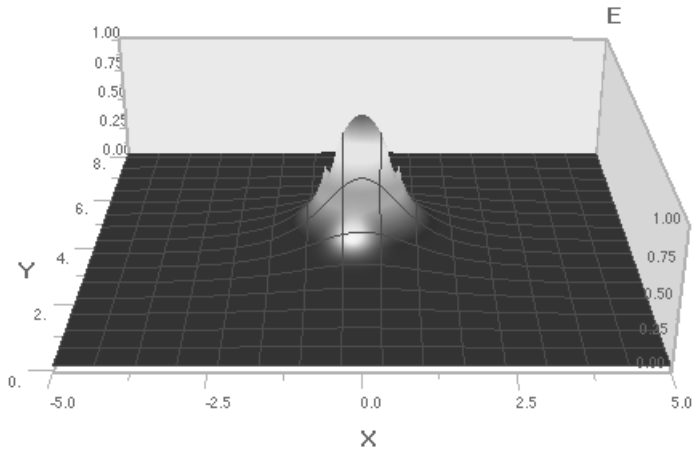

Figure 2. Mode profile of the single mode Si_3N_4/ SiO_2 waveguide.

Accurately measuring waveguide loss is always a challenging task. It is even more challenging for measuring low loss waveguides. Existing techniques include cutback, scattering capture, and Fabry-Perot resonance measurement. The cutback method relies on the consistent coupling to the polished waveguides of different lengths. It is not only time consuming, but also has large uncertainties because the coupling coefficients are not exactly the same from waveguide to waveguide. Scattering capture is based on the assumption that the scattering light is proportional to the intensity inside the waveguide. For low loss buried channel waveguides, there is no scattering light to be observed. The Fabry-Perot resonance method is used to measure low loss waveguides with relatively high reflections from both facets. For silicon nitride waveguides, the reflection from the waveguide facet is less than 4%, the Fabry-Perot resonance is very weak. Therefore, the loss measurement has an intrinsic large uncertainty.

3.1 Lateral mode interference 3 dB splitter

Here we developed a new technique to measure the waveguide device loss, not only for linear waveguides, but also for curved waveguides, tapered waveguides, and waveguide crossing. The new technique relies on lateral mode interference (LMI) 3dB splitter. In theory, a 1X2 LMI with single mode input and outputs should give a perfect 3dB power splitting because of the intrinsic symmetry of the 1X2 LMI waveguide structure. We designed an LMI for a wavelength of 1550nm and put it on the same mask as the PLC structures we were going to measure. The dimension of the LMI was 3.2 micron by 72 micron. Figure 3 (a) shows a simulation of electrical field propagation of the LMI splitter using a beam propagation method (BPM) code. Figure 3 (b) is a scanning electron micrograph (SEM) of the fabricated LMI device. Figure 4 shows the measured splitting ratio of the 1X2 LMI splitter. The horizontal axis is the total power of the two output waveguides. The vertical axis is the ratio of output one over the total power. We intentionally misaligned the coupling of the input waveguide to reduce the total output power. Figure 4 shows that the LMI splitting ratio does not depend on the misalignment. It is because of the nature of the single mode waveguide. We measured three LMI splitters on the same wafer. The splitting ratios fall into the range of {0.49, 0.51}. In terms of dB, the deviation from perfect 3 dB power splitting is less than 0.1 dB in general. When the input coupling is optimized, the deviation from perfect 3 dB power splitting is less than 0.05 dB. Although it is not our

major concern, we measured the insertion loss of the LMI. The insertion loss is about 1.0 dB. The LMI insertion loss measurement is carried out by using a cascade LMI structure as shown in Figure 5. We changed the aspect ratio of the PLC in Figure 5 to see it clearly. The ratio of the sum of I1 and I2 over I3 gives the insertion loss of the LMI splitter.

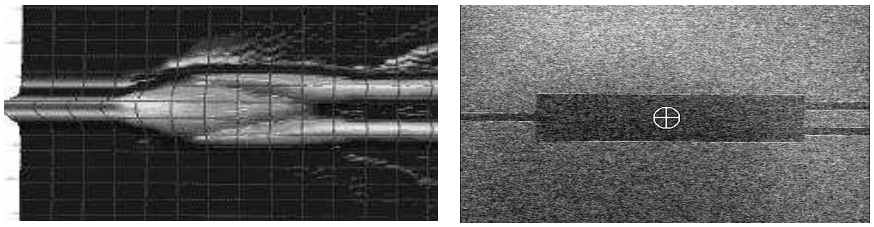

Figure 3. Lateral mode interference (LMI) 3 dB splitter: simulation (left) and fabricated device (right).

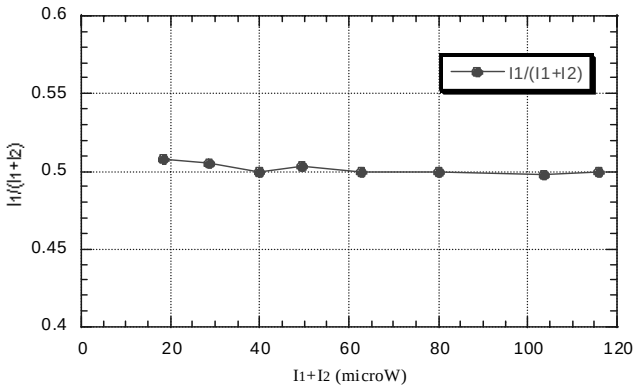

Figure 4. Splitting ratio of the LMI splitter vs. alignment.

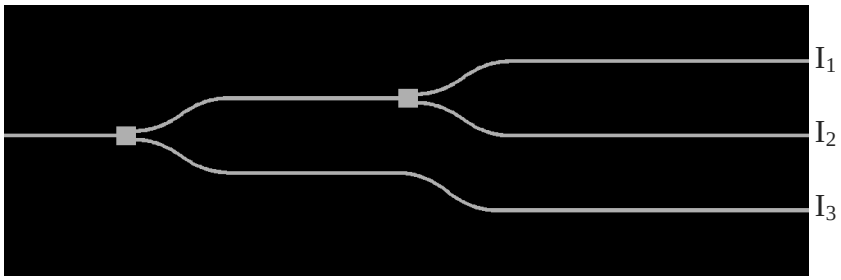

Figure 5. Configuration of cascade LMI 3 dB splitters.

3.2 Straight waveguide loss and bending loss

We used the LMI 3 dB splitter to measure the waveguide linear loss, curvature loss and crossing loss. In order to measure the curvature loss and linear loss, we designed several PLCs as shown in Figure 6. We changed the aspect ratio of the PLCs in order to have better picture of them. In the bottom PLC of Figure 6, a LMI 3dB splitter splits the light into two output waveguides. The lower output waveguide is a straight waveguide. The upper output waveguide

makes four 90° turns with a 500 micron radius of curvature before becoming a straight waveguide. We measured the output powers from the upper and the lower waveguides. The ratio of the power is R_1. In the middle PLC of Figure 6, a LMI 3dB splitter splits the light into two output waveguides. The upper output waveguide is a straight waveguide. The lower output waveguide makes twelve 90° turns before becoming a straight waveguide. We measured the output powers from the lower and the upper waveguides. The ratio of the powers is R_2. In the top PLC of Figure 6, a LMI 3dB splitter also splits the light into two output waveguides. The lower output waveguide is a straight waveguide. The upper output waveguide first makes four 90° turns, then comes straight back (6 mm). It makes another two 90° turns, goes straight forward (8 mm), makes another two 90° turns, and then becomes a straight waveguide. We measured the output powers from the upper and the lower waveguides. The ratio of the powers is R_3. All these turns are curved waveguides of 500 micron radius of curvature. We used the measured ratios of R_1, R_2, R_3 to calculate the linear waveguide loss and bending loss. The best wafer we fabricated had 0.5 dB per cm linear waveguide loss and 0.6 dB per 90° turn bending loss. A previous report has published a loss number of 0.1dB/cm in Si_3N_4/ SiO_2 waveguide[16]. That result has never been repeated. A loss of 0.5dB/cm is among the world best for repeatable Si_3N_4/ SiO_2 waveguide fabrications.

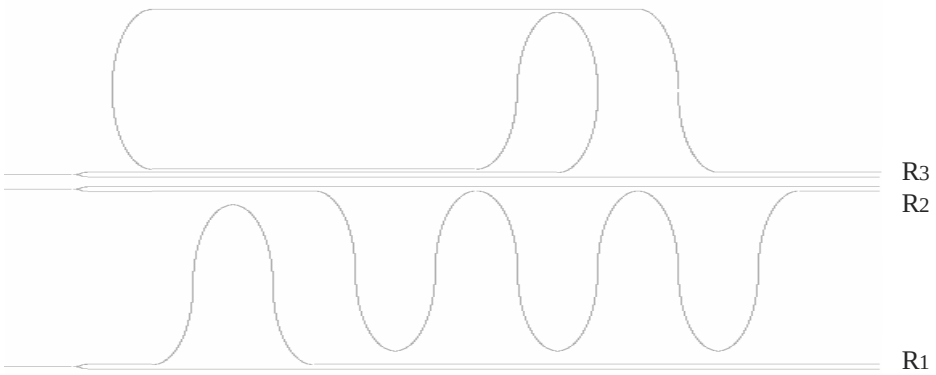

Figure 6. PLCs for waveguide linear loss and curvature loss measurements.

3.3 Waveguide crossing loss

Using a similar technique, we designed waveguide crosses of various widths and measured their crossing losses in their fundamental modes. In our design, we used eight cascade waveguide crosses in order to measure very small waveguide crossing loss. Figure 7 shows the PLC circuit for measuring the waveguide crossing loss. An LMI 3 dB splitter was used to split the light into two output waveguides. The upper waveguide has multiple crosses and the lower waveguide is simply a straight waveguide. We measured the power output ratio (R) between the upper waveguide and the lower waveguide. The transmission of each cross is $R^{1/8}$.

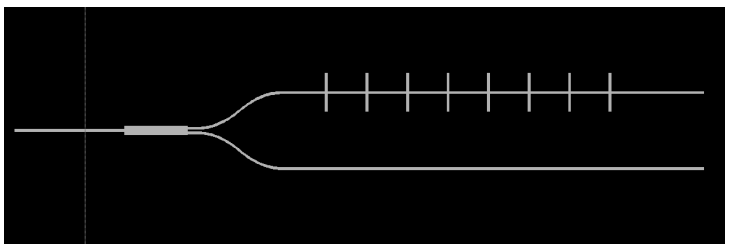

Figure 7. Lightwave circuit measuring the waveguide crossing loss.

To measure the dependence of crossing loss on waveguide width, we used the waveguide taper to taper the waveguide to the desired width included a straight waveguide section with multiple crosses, and then tapered down the waveguide to its original width. In order to get an accurate waveguide loss measurement, we corrected for the insertion losses associated with the waveguide tapers.

We designed and fabricated waveguide crosses of 0.8, 1.2, 1.6, 2.4, and 3.6 micron widths. The crossing regions were squares because the crossing vertical waveguides had the same width as the horizontal waveguide. Figure 8 shows the transmission of these waveguide crosses. The crossing loss is flat when the waveguide width increases from 0.8 to 2.4 micron, and decreases significantly when the waveguide width increases to 3.6 micron. The loss reaches as low as 0.12 dB for the waveguide width of 3.6 micron. The waveguide crossing loss is caused by two mechanisms. One is due to the mode index mismatch in the laterally guided region and the crossing region. In the crossing region, the light loses confinement in the lateral dimension. The mode index is different from the laterally guided region. In the crossing region, the mode profile diverges in the lateral dimension until it reaches the output waveguide. The mode divergence is similar to that of a Gaussian beam diverging in free space. It can be characterized similarly by a Raleigh length[17]. The Raleigh length is the traveling distance where the spot size is 1.414 times the waist spot size. The Raleigh length is proportional to the square of the mode size at its minimum. An approximate fractional power loss (L) of waveguide crossing is given as[18]

$$L \approx \frac{(n_2 - n_1)}{V^2}\left(\frac{\rho_x}{s_x}\right)^2\left(\frac{\rho_y}{s_y}\right)^2 \qquad (1)$$

where ρ_x and ρ_y are the half widths of the waveguide in x and y dimensions, s_x and s_y are the mode size in x and y dimensions. V is the V-number of the wave guide[19]. For wider waveguides, the fundamental mode size is about the same as the waveguide cross section. The V-number dominates the loss. The loss decreases when the waveguide width increases, i.e. V-number increases.

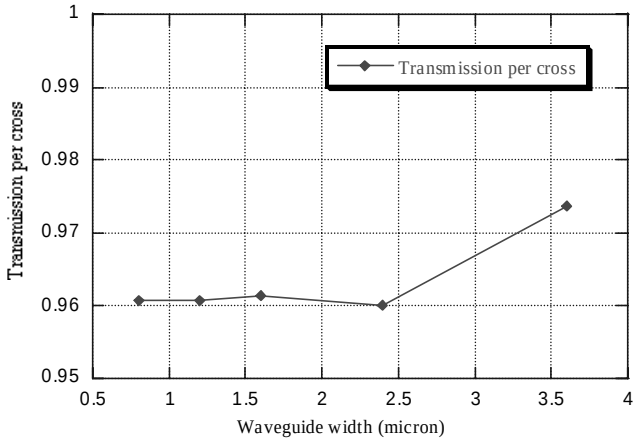

Figure 8. Transmission of waveguide cross vs. the waveguide width.

3.4. Leaky mode waveguide polarizer

A conventional single-mode planar optical waveguide is not truly single mode because it still supports two fundamental modes, i.e. transverse electric (TE) and transverse magnetic (TM) modes. The TE and TM modes can couple together while traveling in the PLC circuits. The capability of keeping one mode and removing another one is very crucial for integrated photonic sensor applications.

An integrated waveguide polarizer can be realized in several techniques. One technique is to deposit a thin metal layer on the top cladding of the waveguide[20]. The TM polarization mode will couple to the surface plasmon wave and damp the energy to the metal layer. The attenuation of the TE mode is only caused by the absorption of the

metal layer. It can be minimized in the design. Another technique for making waveguide polarizer is to use a polarization directional coupler[21]. A polarization directional coupler is a directional coupler that separates two polarization modes into two outputs. A simpler technique for making a waveguide polarizer is to use a leaky mode waveguide. By designing the cross section of the waveguide and choosing a proper lower cladding thickness, the TM mode can be a strong leaky mode due to the waveguide tunneling into the high index silicon substrate while keeping TE mode leakage negligible.

We have fabricated a leaky-mode waveguide polarizer that can effectively remove the TM mode and keep the TE mode at the same time. The waveguide consists of an elongated rectangular shape waveguide core of 1.2 X 0.15 micron^2 and a lower silica cladding of 3.5 micron. The elongated design of the waveguide cross section makes the TM mode much bigger than the TE mode. Therefore, the energy of the TM mode can significantly leak into the high refractive index silicon substrate through waveguide tunneling. Figure 9 shows the TE polarization mode and TM polarization mode profile in the waveguide. Figure 10 is the calculated propagation loss of the TE and TM modes in that waveguide. TM mode loss is significantly larger than the TE mode loss because of the higher leakage to the silicon wafer substrate, particularly for thinner lower cladding thicknesses. The calculated polarization extinction ratio for 3.5 micron lower cladding is about 65 dB/ cm. The calculated polarization extinction ratio for 3.8 micron lower cladding is about 50 dB/cm.

Figure 9. The TE mode (left) and TM mode (right) of the waveguide.

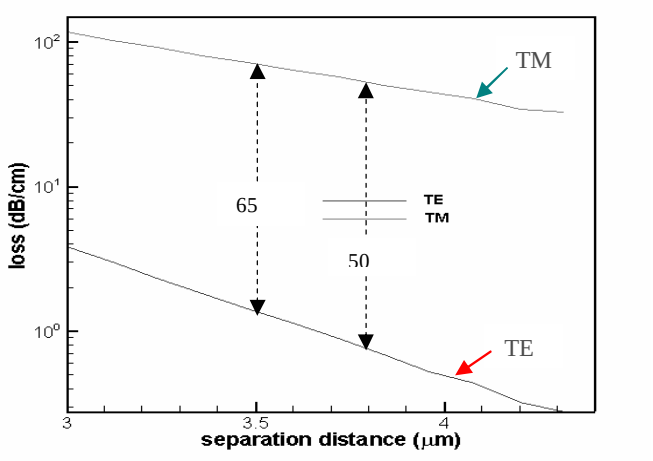

Figure 10. The TE mode and TM mode losses vs. thickness of lower cladding layer.

In our experiment, the loss of the TM mode is so high that the TM mode is almost immeasurable for 1 cm straight waveguide. We used a cutback method to measure the losses of TE and TM modes. As we discussed earlier, the cutback method has a large uncertainty range. But since the loss difference between the TM mode and the TE mode is so much bigger, the polarization extinction ratio we get is quite reliable. The TE mode loss is about 1dB/cm with

an uncertainty of 0.5dB/cm, and the TM mode has a loss of 46 dB/cm with an uncertainty of 1 dB/cm. Therefore, the leaky mode waveguide polarizer has a polarization extinction ratio of 45dB/cm with an uncertainty of 2dB/cm. Figure 11 shows the TE mode and the TM mode of the waveguide after traveling along a 0.5 cm long waveguide section with about the same input optical power. The pictures were captured by a Hamamatsu lead sulfide tube IR camera. Since the input couplings are different for the TE and TM modes and the brightness of the camera is nonlinearly related to the intensity of light, the pictures shown in Figure 11 do not have any quantitative information.

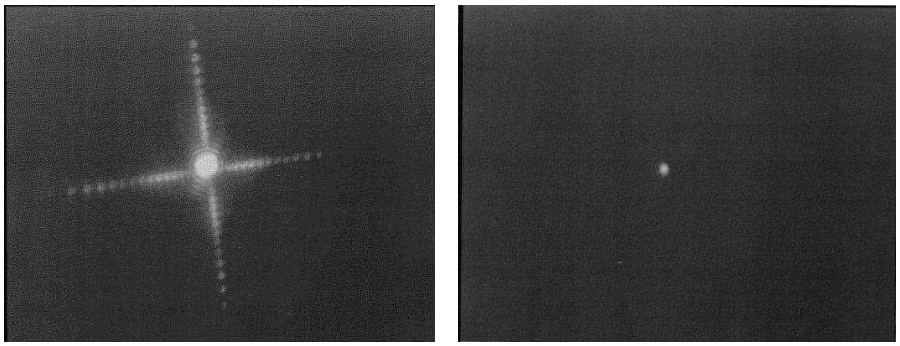

Figure 11. The TE mode (left) and TM mode (right) of the waveguide.

4. WAVEGUIDE RING RESONATOR

The large refractive index contrast between the silicon nitride core and the silicon dioxide cladding allows the waveguide to have small turns with low radiation bending loss. Low bending loss can help make high-Q waveguide ring resonators. High-Q waveguide ring resonators have applications for photonic sensors wavelength add/drop filters, and optical switches. A lot of interesting integrated photonic devices can be built by using ring resonators.

The transmission of a high-Q ring resonator coupled straight waveguide is very sensitive to the perturbation of its optical path length. A slight change of mode index can cause a significant change in the transmission signal. One application is to make an evanescent wave biochemical sensor based on a high-Q ring resonator.

Figure 12 shows a ring coupled Mach-Zender interferometer. One arm of the Mach-Zender interferometer is coupled with a ring resonator. The top cladding of the ring is thinned so that the evanescent wave extends into the air. Once biochemical agents attach to the top thin cladding of the ring, the mode index of the waveguide ring will change. A large optical phase delay will be induced by the ring due to the resonance enhancement.

Figure 13 shows the transmission of the Mach-Zender interferometer as a function of the effective mode index in the ring. We assume that loss in the ring is 2dB/cm, the coupling from the straight waveguide to the ring is 20%, and the wavelength is 1.55 micron. The radius of the ring is 200 micron. Currently, we are working on design and fabrication of evanescent waveguide rings for bio-photonic sensor application. The challenge is to make rings with low loss and high Q-factor.

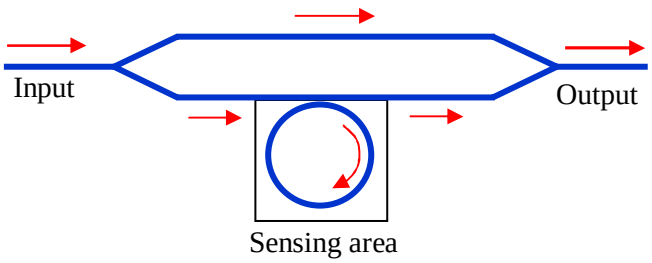

Figure 12. Ring resonator coupled Mach-Zender interferometer.

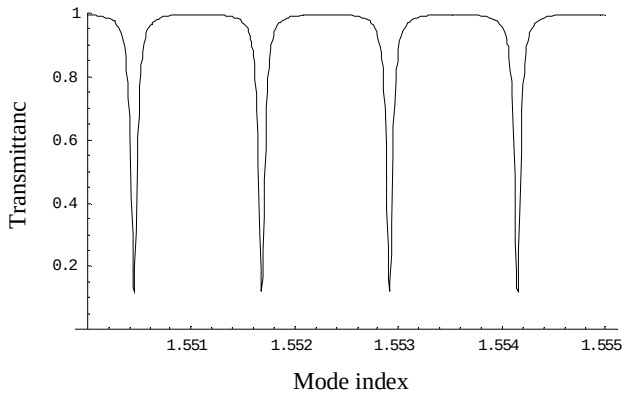

Figure 13. Transmission of a ring resonator coupled Mach-Zender interferometer.

5. SUMMARY

We designed, fabricated, and characterized several PLC devices with Si_3N_4/SiO_2 materials on silicon substrates. We used a new technique to accurately measure the losses of these devices, particularly for low waveguide crossing losses. We achieved 0.5dB/cm linear waveguide loss and 0.12 dB per cross waveguide crossing loss. A 0.5dB/m loss is among the world best for repeatable Si_3N_4/SiO_2 waveguide fabrications. The crossing loss of 0.12dB is the lowest cross loss ever measured and reported. We also demonstrated a leaky mode waveguide polarizer with 45dB/cm polarization extinction ratio between the TE and the TM modes. Finally, we discussed the Si_3N_4/SiO_2 waveguide ring resonator and its application for integrated photonic biochemical sensors.

ACKNOWLEDGMENTS

This work supported by the U. S. Department of Energy under contract DE-AC04-94AL85000. Sandia is a multiprogram laboratory operated by Sandia Corporation, a Lockheed Martin Company, for the United States of Department of Energy's National Nuclear Security Administration under contract DE-AC04-94AL85000.

REFERENCES

1. A. Hymen, K. Kato, and T. Maya, "Silicon-based planar lightwave Circuits," *IEEE Journal of Selected Topics in Quantum Electronics*, **4**, p. 913, 1998.
2. R. M. de Ridder, K. Worhoff, A. Driessen, P. V. Lambeck, and H. Albers, "Silicon Oxynitride planar waveguide structures for application in optical communication," *IEEE Journal of Selected Topics in Quantum Electronics*, **4**, p. 930, 1998.
3. D. A. P. Pulla, B. V. Borges, M. A. Romero, N. I. Morimoto, and L. G. Neto, "Design and fabrication of SiO_2/Si_3N_4 integrated optics waveguides on silicon substrates," *IEEE Transactions on Microwave Theory and Techniques*, **50**, p. 9, 2002.
4. D. Cristea, F. Craciunoiu, M. Modreanu, M. Caldararu, I. Cernica, "Photonic circuits integrated with CMOS compatible photodetectors," *Optical Materials*, **17**, pp. 201-205, 2001.
5. C. E. Chryssou, F. Di Pasquale, C. W. Pitt, "Er3+-doped channel optical waveguide amplifiers for WDM systems: a comparison of telluride, alumina and Al/P silicate materials," *IEEE Journal on Selected Topics in Quantum Electronics*, **6**, pp. 114 – 121, 2000.
6. S. Chan, P. M. Fauchet, "Silicon microcavity light emitting devices," *Optical Materials*, **17**, pp.31-34, 2001.
7. G. Barillaro, F. Pieri, U. Mastromatteo, *Optical Materials*, **17**, pp. 91-94, 2001.

8. L. Pavesi, "A review of the various efforts to a silicon laser," *Proceedings of SPIE-The International Society for Optical Engineering*, **4997**, pp.206-220, 2003.
9. S. Coffa, S. Libertino, G. Coppola, A. Cutolo, "Feasibility analysis of laser action in erbium-doped silicon waveguides," *IEEE Journal of Quantum Electronics*, **36**, pp.1206-1213, 2000.
10. L. Pavesi, "Will silicon be the photonic material of the third millenium?" *Journal of Physics: Condensed Matter*, **15**, p.R1169, 2003.
11. R. Adar, M. R. Serbin, V. Mizrahi, "Less than 1 dB per meter propagation loss of silica waveguides measured using a ring resonator," *Journal of Lightwave Technology*, **12**, pp. 1369-1372, 1994.
12. K. K. Lee, D. R. Lim, Luan Hsin-Chiao, A. Agarwal, J. Foresi, L. C. Kimerling, "Effect of size and roughness on light transmission in a Si/SiO_2 waveguide: Experiments and model," *Applied Physics Letters*; **77**, p.1617, 2000.
13. K. K. Lee, D. R. Lim, L. C. Kimerling, J. Shin, J. F. Cerrina, "Fabrication of ultralow-loss Si/SiO_2 waveguides by roughness reduction," *Optics Letters*, **26**, p. 1888, 2001.
14. G. Bona, W. E. Denzel, B. J. Offrein, R. Germann, H. W. M. Salemink, F. Horst, "Wavelength division multiplexed add/drop ring technology in corporate backbone networks," *Optical Engineering*, **37**, p.3218, 1998.
15. C. H. Henry, R. F. Kazarinov, H. J. Lee, K. L. Orlowsky, and L. E. Katz, "Low loss Si3N4- SiO2 optical waveguide on Si," *Applied Optics*, **vol. 26**, p. 2621, 1987.
16. S. Dutta, H. E. Jackson, J. T. Boyd, R. L. Davis, and F. S. Hickernell, "CO_2 laser annealing of Si_3N_4, $N_{b2}O_5$, and Ta_2O_5 thin film optical waveguides to achieve scattering loss reduction," *IEEE Journal of Quantum Electronics*, **QE-18**, p. 803, 1982.
17. B. A. Saleh and M. C. Teich, "*Fundamentals of Photonics,"* p. 83, A Wiley –Interscience Publication, New York, 1991.
18. F. Ladouceur and J. D. Love, *"Silica-based buried channel waveguides and devices,"* p. 167, Chapman & Hall, New York, 1996.
19. F. Ladouceur and J. D. Love, *"Silica-based buried channel waveguides and devices,"* p. 17, Chapman & Hall, New York, 1996.
20. G. Grand, S. Valette, "Optical polarisers of high extinction ratio integrated on oxidised silicon substrate," *Electronics Letters*, **20**, p.730, 1 984.
21. H. Nishihara, M. Haruna, T. Suhara, *Optical Integrated Circuits*, p. 258, McGraw-Hill Book Company, New York, 1987.

*Junpeng Guo, Sandia National Laboratories, P.O. Box 5800, MS 0603, Albuquerque, NM 87185; phone: (505) 284 9715, jguo@sandia.gov